

# Connexin46 Is Retained as Monomers in a *trans*-Golgi Compartment of Osteoblastic Cells

Michael Koval, James E. Harley, Elizabeth Hick, and Thomas H. Steinberg

Department of Medicine, Department of Cell Biology and Physiology, Washington University School of Medicine, St. Louis, Missouri 63110

**Abstract.** Connexins are gap junction proteins that form aqueous channels to interconnect adjacent cells. Rat osteoblasts express connexin43 (Cx43), which forms functional gap junctions at the cell surface. We have found that ROS 17/2.8 osteosarcoma cells, UMR 106-01 osteosarcoma cells, and primary rat calvarial osteoblastic cells also express another gap junction protein, Cx46. Cx46 is a major component of plasma membrane gap junctions in lens. In contrast, Cx46 expressed by osteoblastic cells was predominantly localized to an intracellular perinuclear compartment, which appeared to be an aspect of the TGN as determined by immunofluorescence colocalization. HeLa cells transfected with rat Cx46 cDNA (HeLa/Cx46) assembled Cx46 into functional gap junction channels at the cell surface. Both rat

lens and HeLa/Cx46 cells expressed 53-kD (nonphosphorylated) and 68-kD (phosphorylated) forms of Cx46; however, only the 53-kD form was produced by osteoblasts. To examine connexin assembly, monomers were resolved from oligomers by sucrose gradient velocity sedimentation analysis of 1% Triton X-100-solubilized extracts. While Cx43 was assembled into multimeric complexes, ROS cells contained only the monomer form of Cx46. In contrast, Cx46 expressed by rat lens and HeLa/Cx46 cells was assembled into multimers. These studies suggest that assembly and cell surface expression of two closely related connexins were differentially regulated in the same cell. Furthermore, oligomerization may be required for connexin transport from the TGN to the cell surface.

**G**AP junction channels mediate intercellular communication by allowing the direct transfer of ions and small aqueous molecules between neighboring cells. Gap junction channel proteins, or connexins, have been identified with sizes in the range of 26–56 kD (for reviews see 6, 7, 17, 21, 32). Channels composed of different connexins have distinct properties, and most tissues express more than one connexin. There is increasing evidence that multiple connexins can interact to form heteromeric gap junction channels (25, 52).

Regulation at the level of gene expression is clearly one important way that gap junction composition can be regulated (5, 10, 12, 14, 31, 50, 58). Connexin transport and assembly into gap junction channels are other possible points where cells can regulate the formation of gap junction

channels (17, 38). A number of studies have shown that newly synthesized connexins are transported through the normal secretory apparatus (18, 39, 40, 46). However, in contrast with most multimeric membrane protein complexes that are formed in the ER (3, 13, 28), the identity of the site of connexin oligomerization remains controversial (32). Both ER (33) and Golgi apparatus (41) have been suggested as sites for connexin assembly into gap junction channels or hemichannels.

In previous studies we have examined the expression of connexins in human and rat osteoblastic cells (11, 30, 53). All of the cells examined express Cx43 ( $\alpha_1$ ) in junctional plaques at the cell surface. In addition, some osteoblasts also produce Cx45 ( $\alpha_6$ ), which also shows plasma membrane localization (53). In this paper we have characterized a third endogenous connexin expressed by rat osteoblastic cells, Cx46 ( $\alpha_3$ ).

Cx46 expression has typically been associated with plasma membrane gap junction channels in lens (14, 22, 25, 29, 43, 49, 57). We found that Cx46 was expressed by primary rat osteoblastic cells and two osteosarcoma cell lines, ROS-17/2.8 (ROS) and UMR 106-01 (UMR) cells. In contrast with Cx43 and Cx45, Cx46 was largely retained in an intracellular perinuclear compartment. Little, if any, Cx46 accumulated on the cell surface, as determined by immunofluorescence microscopy. Instead, Cx46 was re-

Please address all correspondence to Michael Koval, Department of Medicine, Washington University School of Medicine, Campus Box 8051, 660 S. Euclid Avenue, St. Louis, MO 63110. Tel.: (314) 362-6606. Fax: (314) 362-9230. e-mail: koval@id.wustl.edu

As of July 1, 1997, M. Koval's address is Institute for Environmental Medicine and Department of Physiology, University of Pennsylvania School of Medicine, 1 John Morgan Building, 3620 Hamilton Walk, Philadelphia, PA 19104.

tained in a *trans*-aspect of the Golgi apparatus, probably the TGN. In contrast, we found that HeLa cells stably transfected with rat Cx46 (HeLa/Cx46) formed functional gap junction channels by Cx46 at the plasma membrane.

In addition to the differential transport of Cx43 and Cx46 by ROS cells, these cells also showed differences in connexin assembly. While Cx43 was assembled into hexameric gap junction hemichannels by ROS cells, the intracellular pool of Cx46 remained as unassembled monomers. Thus, transport and assembly of Cx43 and Cx46 are differentially regulated by osteoblastic cells. These data are discussed in the context of potential roles for connexin oligomerization in the regulation of transport.

## Materials and Methods

### Cells

ROS 17/2.8 and UMR 106-01 cells were cultured in MEM (No. 11095-056; GIBCO BRL, Gaithersburg, MD) containing 10% heat-inactivated bovine calf serum (BCS)<sup>1</sup> (Hyclone, Logan, UT), 2 mM glutamine, 1 mM sodium pyruvate, 1% nonessential amino acids (GIBCO BRL), 5 U/ml penicillin, and 5 µg/ml streptomycin (MEM + BCS). Primary osteoblastic cells were isolated from fetal rat calvaria as previously described (51) and cultured in MEM + BCS for no more than six passages. HeLa cells were kindly provided by Jeanette Pingle and Matthew Thomas (Washington University, St. Louis, MO).

### RNA Blots

Total cellular RNA was isolated using guanidium isothiocyanate and probed for rat Cx46 and human  $\gamma$ -actin as previously described (30).

### Antibodies

A number of immunological reagents were generous gifts from the following researchers. Tissue-culture supernatant from murine hybridoma cells producing anti-Cx50 (MP70;  $\alpha_8$ ) was from Drs. J. Kistler (University of Auckland, New Zealand) and D. Goodenough (Harvard University, Boston, MA) (14, 15). Tissue-culture supernatant containing monoclonal murine anti-rat TGN38 was from Dr. G. Banting (University of Bristol, UK) (24). Production of rabbit polyclonal antiserum that recognizes Cx43 was previously described (4).

Rabbit anti-Cx46 IgG was produced using a 6His-tagged Cx46 fusion protein. A cDNA consisting of the COOH-terminal tail sequence of rat Cx46 was produced by PCR amplification using a full-length rat Cx46 cDNA as a template (sense primer: 5'-CGAGA GCGAC ATATG CTAGA GATT ACCAC CT-3'/antisense primer: 5'-AGCGA GCGGA TCCTT TCTAC CTGTT GATTT GA-3'). The resulting PCR product was amplified and inserted into the pET-15b vector (Novagen, Madison, WI) to produce a bacterial expression vector containing cDNA encoding for a fusion protein containing the Cx46 COOH terminus, a thrombin cleavage site, and six histidine residues (Cx46-his). Bacterial expression of Cx46-his was induced by treatment with isopropylthio- $\beta$ -D-galactoside, cell extracts were prepared, and Cx46-his was affinity purified using a nickel/His-Bind chelation resin column (Novagen). This product was used to induce polyclonal antiserum in rabbits by established protocols.

Polyclonal serum that recognized Cx46 was initially identified by immunoblot analysis of rat lens total protein preparations that showed reactive bands with the expected  $M_r$  at 53 and 68 kD, consistent with previous reports (26, 29, 57). Preincubation of anti-Cx46 antiserum with antigen eliminated binding to both bands in samples prepared from lens and ROS cells (see Fig. 3, lanes 2 and 4). The perinuclear staining pattern obtained for osteoblasts labeled with anti-Cx46 (e.g., see Fig. 2) was eliminated by preincubation of the antiserum with Cx46-his protein (not shown). Also, cells that do not express Cx46 did not show any labeling by immunofluorescence or immunoblotting (see Fig. 4).

1. Abbreviations used in this paper: BCS, bovine calf serum; BFA, brefeldin A; NRK, normal rat kidney; PVDF, polyvinylidene difluoride.

## Immunofluorescence Microscopy

Cells were initially cultured on glass coverslips for 1–3 d before examination. The cells were washed twice in PBS, and then fixed and permeabilized for 2 min at room temperature using methanol/acetone (1:1). The cells were washed once with PBS containing 0.5% Triton X-100 and then twice with PBS containing 0.5% Triton X-100 and 2% heat-inactivated normal goat serum (PBS/TX/HIGS). The cells were then incubated with primary antiserum diluted to optimal titer in PBS/TX/HIGS for 45–60 min at room temperature. After washing three times with PBS/TX/HIGS, the cells were further incubated with fluorescent anti-IgG diluted in PBS/TX/HIGS for 45–60 min. The cells were then washed and viewed by fluorescence microscopy using appropriate optics. For Cx46 labeling, anti-Cx46 antiserum was diluted 1:1,000 into PBS/TX/HIGS, and the secondary antiserum was rhodamine-conjugated goat anti-rabbit IgG (Boehringer Mannheim Biochemicals, Indianapolis, IN) diluted 1:500 in PBS/TX/HIGS. For double labeling experiments, Cx43 was labeled using monoclonal antiserum from Zymed Laboratories (South San Francisco, CA), and staining with fluorescent lectins was substituted for labeling with antisera to visualize some organelles. In some instances, images were obtained with a Bio-Rad MRC-1000 confocal fluorescence microscopy system (Hercules, CA); all other images were obtained by epifluorescence microscopy using a Zeiss Axioscope (Thornwood, NY) and GIPSSPC image processing system (Georgia Instruments, Roswell, GA).

## Protein Preparation and Immunoblotting

Total cell protein samples were prepared as previously described (30) and resolved by SDS-PAGE using standard methods and 10% polyacrylamide gels. The proteins were then electrophoretically transferred to polyvinylidene difluoride (PVDF) membranes (transfer buffer: 50 mM Tris, 380 mM glycine, 0.025% (wt/vol) SDS, 20% MeOH), blocked with blotto (40 mM Tris, 5% (wt/vol) Carnation powdered milk, 0.1% (vol/vol) Tween-20) for 1 h at room temperature, and then blocked overnight with antiserum diluted into blotto. The membranes were then washed, and specific bands were detected using HRP-conjugated goat anti-rabbit IgG (Tago, Burlingame, CA) and enhanced chemiluminescence (ECL; Amersham Intl., Little Chalfont, UK). Cx50 immunoblots were detected using peroxidase-conjugated goat anti-mouse IgG + IgM (Boehringer Mannheim Biochemicals). After a series of exposures, films showing unsaturated bands were digitized and quantitated using an image analysis system (Georgia Instruments).

## Sucrose Gradient Velocity Centrifugation

This procedure was adapted from that of Musil and Goodenough (40). Cells cultured for 1–3 d in 100-mm tissue-culture dishes were washed twice with PBS, and then scraped into PBS at 4°C and centrifuged at 500 g for 5 min. The cell pellet was resuspended in 2.75 ml incubation buffer (0.14 M NaCl, 5.3 mM KCl, 0.35 mM Na<sub>2</sub>PO<sub>4</sub>, 0.35 mM KH<sub>2</sub>PO<sub>4</sub>, 0.8 mM MgCl<sub>2</sub>, 2.7 mM Hepes, pH 7.4) containing protease (10 mM *N*-ethylmaleimide, 1 mM phenylmethylsulfonylchloride, 2 µg/ml leupeptin, 1 µg/ml pepstatin) and phosphatase inhibitors (1 mM NaVO<sub>4</sub>, 10 mM NaF) at 4°C and homogenized with a ball-bearing cell homogenizer (1). The preparation was then centrifuged at 500 g for 5 min to obtain a postnuclear supernatant and brought to 1% Triton X-100. After a 30-min incubation at 4°C,

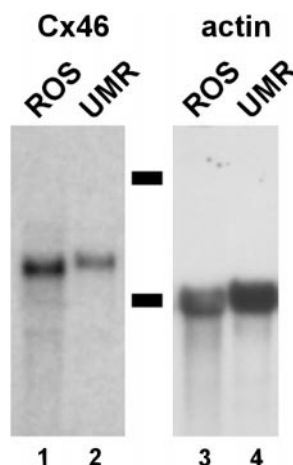
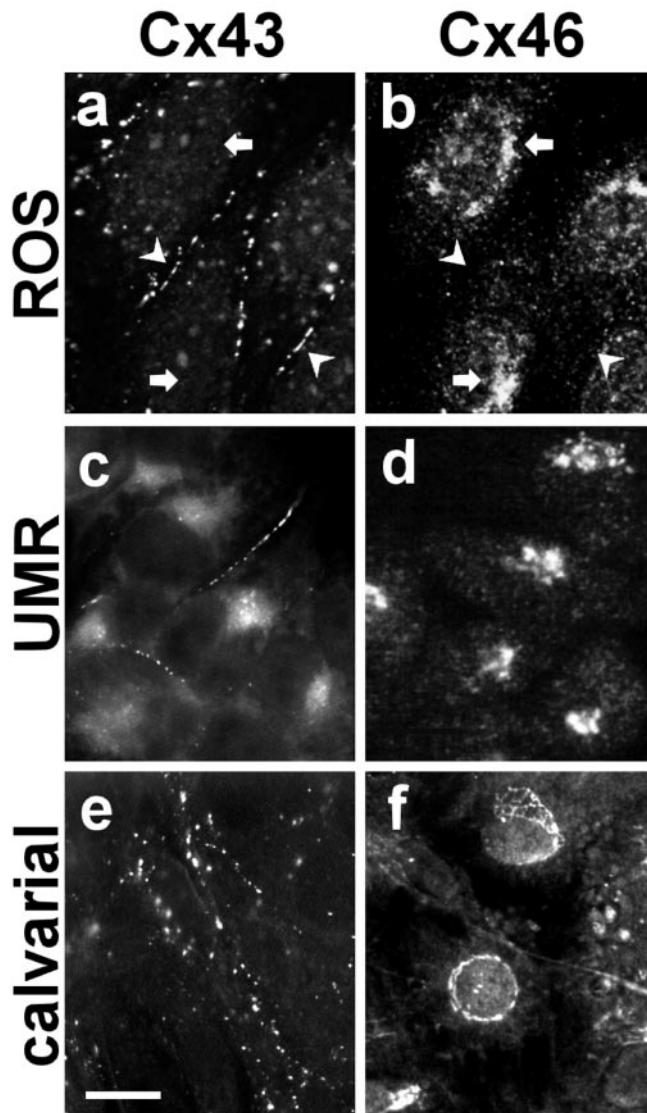
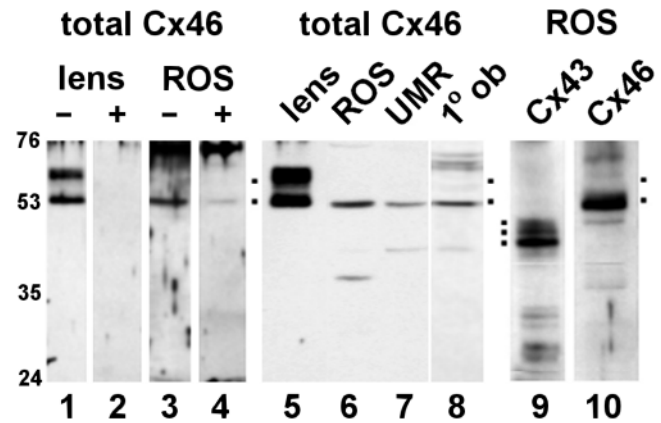


Figure 1. Northern blot analysis of Cx46 mRNA. Total RNA was isolated from either ROS (lanes 1 and 3) and UMR (lanes 2 and 4) cells, subjected to agarose gel electrophoresis, transferred to membranes, and then hybridized with a radiolabeled cDNA probe for Cx46 (lanes 1 and 2). The membranes were then stripped and reprobbed for actin as a control for mRNA loading (lanes 3 and 4). Dashes correspond to 28S and 18S rRNA.



**Figure 2.** Intracellular distribution of Cx46 in osteoblasts. (*a* and *b*) Colocalization. ROS cells on glass coverslips were fixed, permeabilized, and double immunolabeled with monoclonal anti-Cx43 mouse IgG and polyclonal anti-Cx46 rabbit IgG. The cells were then labeled with rhodamine-conjugated goat anti-mouse IgG and FITC-conjugated goat anti-rabbit IgG to visualize Cx43 (*a*) and Cx46 (*b*) by confocal microscopy. (*Arrowheads*) Cx43 localized to the cell surface; (*arrows*) Cx46 in the perinuclear region of the cell. (*c–f*) Single label localization. UMR cells (*c* and *d*) or rat calvarial cells (*e* and *f*) on glass coverslips were fixed, permeabilized, and immunolabeled with either anti-Cx43 (*c* and *e*) or anti-Cx46 (*d* and *f*) antiserum and rhodamine-conjugated goat anti-rabbit IgG. *c–f* were obtained by epifluorescence microscopy. These cells also show the characteristic perinuclear accumulation of Cx46. Note that the immunofluorescence shown in *c* represents an area showing very high levels of Cx43 expression by UMR cells. Bar, 10  $\mu$ m.

the sample was centrifuged at 100,000 *g* for 30 min to remove Triton-insoluble material, and then layered onto a 3.6-ml 5–20% sucrose gradient in incubation buffer + 0.1% Triton X-100 on top of a 0.2-ml 25% sucrose cushion. Samples from intact lens were treated in a similar manner, except that they were minced with a razor blade and incubated in 1% Triton X-100 for 12 h. The gradient was centrifuged using an SW55 rotor in a model L7-55 ultracentrifuge (Beckman Instruments, Inc., Palo Alto, CA) for 16 h at 148,000 *g*. After centrifugation, samples were collected from the bottom of



**Figure 3.** Immunoblot for Cx46 in lens and osteoblasts. (*Lanes 1–4*) Samples from rat lens (*lanes 1* and *2*) and ROS (*lanes 3* and *4*) were resolved by SDS-PAGE, electrophoretically transferred to PVDF membranes, and then immunoblotted for Cx46. For *lanes 2* and *4*, the antiserum was preincubated with Cx46-his before immunoblotting, which blocked the recognition of Cx46. (*Lanes 5–8*) Samples from rat lens (*lane 5*), ROS (*lane 6*), UMR (*lane 7*), and primary rat calvarial cells (*lane 8*) were normalized for total protein and immunoblotted for Cx46. All three osteoblastic cell types expressed the 53-kD form of Cx46. (*Lanes 9* and *10*) Samples from ROS cells corresponding to total cell protein were immunoblotted for either Cx43 (*lane 9*) or Cx46 (*lane 10*). Roughly 10-fold more protein was loaded for these lanes than the corresponding sample in *lane 6*. Migration of molecular weight standards is indicated in the figure, and dots correspond to specific protein bands.

the tube and diluted 1:1 with denaturing SDS sample buffer. Connexins were detected by immunoblotting as described above.

### Immunoprecipitation

ROS cells were incubated in methionine-deficient MEM containing 10% dialyzed BCS for 1 h at 37°C, and then labeled for 5 h at 37°C with 300  $\mu$ Ci per dish  $^{35}$ S-Trans label (ICN Pharmaceuticals, Costa Mesa, CA). The cells were then harvested, and Triton X-100-soluble and -insoluble fractions were prepared as described above. The insoluble pool was resuspended, both fractions were diluted with PBS containing 0.25% BSA and 0.2% gelatin, and SDS was added to 0.5% final concentration. The samples were precleared with protein A-Sepharose and preimmune serum for 90 min at room temperature, and then incubated overnight with specific antiserum and protein A-Sepharose that was preblocked with BSA and gelatin. The beads were washed, resuspended in reducing SDS-PAGE sample buffer, and heated to 68°C to release proteins associated with the beads.

### Transfection

Rat Cx46 cDNA was excised with EcoRI and inserted into the expression vector pSFFVneo (8). Cx46/pSFFVneo was transfected into Hela cells by calcium phosphate precipitation. The cells were incubated overnight at 37°C, and then shocked by treatment with 15% glycerol for 2 min. The cells were then washed and plated in selective medium containing 1 mg/ml G-418. Clones of G-418-resistant cells expressing Cx46 were identified by immunofluorescence and immunoblotting.

## Results

### Cx46 Is Expressed by Osteoblasts

By Northern blot analysis, both ROS and UMR cells were found to express Cx46 mRNA (Fig. 1). The intracellular distribution of Cx43 and Cx46 was examined by indirect

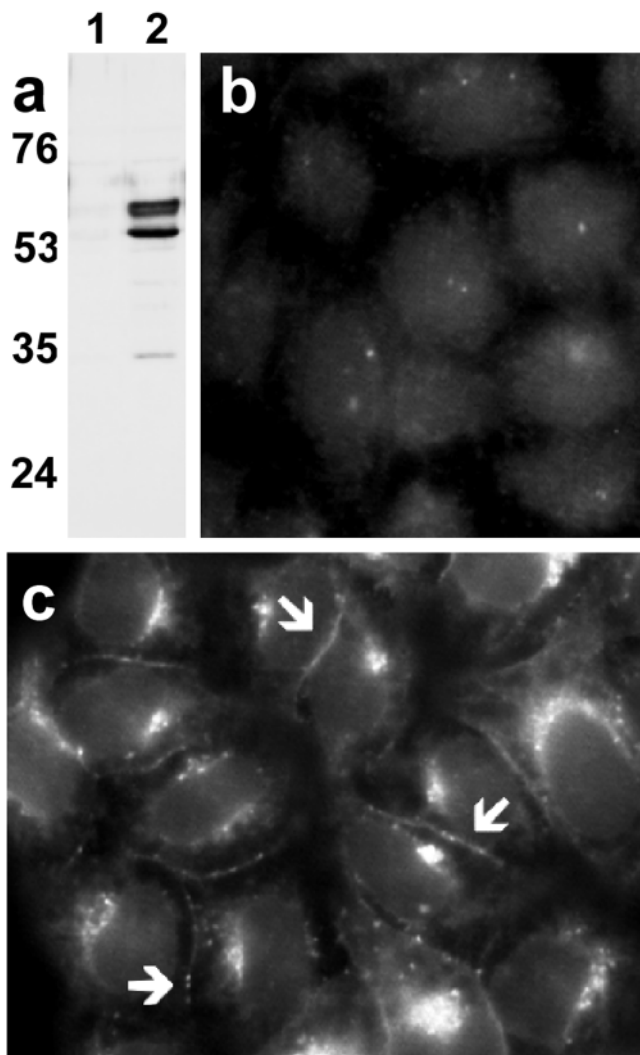


**Figure 4.** Expression of Cx46 by transfected Hela cells. (a) Samples corresponding to Hela cells (lane 1) and Hela/Cx46 cells (lane 2) were normalized for total protein, resolved by SDS/PAGE, electrophoretically transferred to PVDF, and then immunoblotted for Cx46. Faint nonspecific bands present in both lanes are also observed in Western blots using preimmune serum (not shown). (b and c) Untransfected Hela cells (b) or Hela/Cx46 cells (c) plated on glass coverslips were fixed, permeabilized, and then immunolabeled with anti-Cx46 and rhodamine-conjugated goat anti-rabbit IgG. Both images were obtained using the same exposure conditions. Hela/Cx46 cells showed Cx46 present both on the cell surface (arrows) and in the perinuclear region of the cell.

immunofluorescence (Fig. 2). Consistent with our previous work (30, 53), ROS and primary rat calvarial cells showed high levels of Cx43 expression localized to areas where the cells were in close contact, corresponding to gap junctions. While UMR cells express relatively low levels of Cx43 as compared with ROS cells (53), we were able to locate areas where Cx43 was immunolocalized to the cell surface (Fig. 2 c). In contrast, all three cell types showed expression of Cx46. In each case, Cx46 was predominantly localized to an intracellular compartment in the perinuclear region of the cell.

Lens cells typically show the highest levels of Cx46 expression (14, 22, 25, 29, 43, 49, 57). When total lens protein

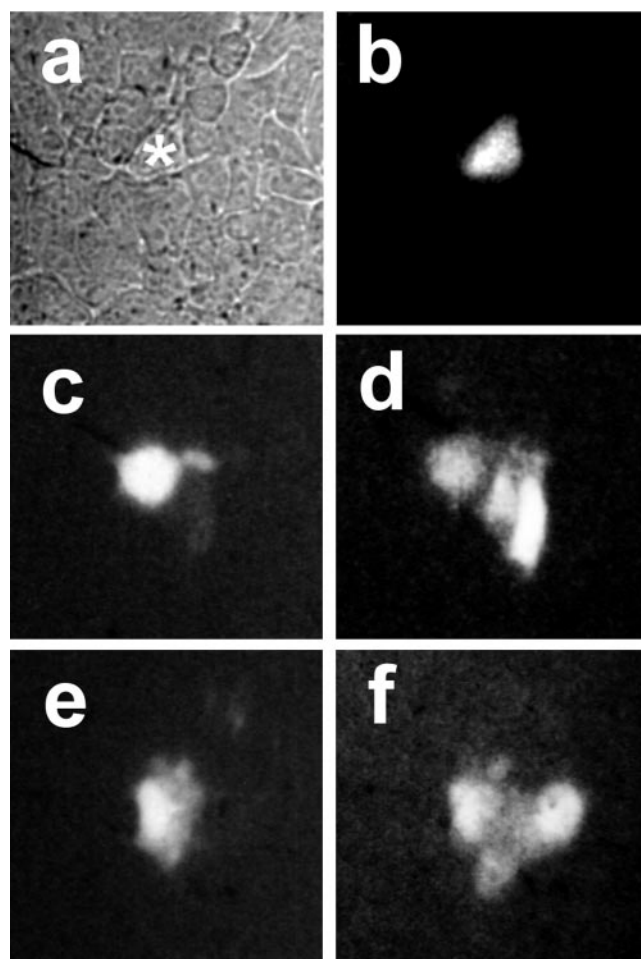


**Figure 5.** Dye transfer by Hela/Cx46 cells. Untransfected Hela cells and Hela/Cx46 cells were cultured on glass coverslips. (a and b) Phase-contrast (a) and fluorescence (b) images of one non-transfected Hela cell in a monolayer that was microinjected with 10 mg/ml Lucifer yellow (\*). Hela cells showed no intercellular transfer of Lucifer yellow. (c–f) Hela/Cx46 cells were microinjected with a mixture of 10 mg/ml Lucifer yellow and 5 mg/ml Texas red ovalbumin. While Texas red was retained in the microinjected cell (c and e), Hela/Cx46 cells showed intercellular transfer of Lucifer yellow to some nearest neighbors (d and f).

extracts were examined by Western blotting, two forms of Cx46 were found with  $M_r$  of 68 and 53 kD (Fig. 3, lanes 1 and 5). This is consistent with previous reports, where the 68-kD band corresponds to a phosphorylated form of Cx46 (26, 29) and may also have other posttranslational modifications (29). In contrast, immunoblots of total proteins isolated from ROS, UMR, and primary osteoblastic cells derived from rat calvaria showed that these cells expressed only the 53-kD form of Cx46. This finding suggests that Cx46 expressed by osteoblastic cells is likely to be nonphosphorylated, although low levels of Cx46 phosphorylation cannot be ruled out. Osteoblasts do not show a general deficiency in connexin phosphorylation, since multiple forms of Cx43 corresponding to phosphorylated species were observed in immunoblots of total protein samples from ROS cells (Fig. 3, lane 9) (38, 39). Also, ROS cells showed qualitatively similar amounts of Cx43 and

Cx46 expression, as determined by immunoblotting (Fig. 3, lanes 9 and 10).

Elfgang et al. (16) found that HeLa cells were highly deficient in connexin expression. We confirmed by Western blotting and immunofluorescence that wild-type HeLa cells did not express Cx46 (Fig. 4), Cx43, or Cx50 (not shown). Thus, HeLa cells were stably transfected with rat Cx46 cDNA (HeLa/Cx46) to examine the targeting of Cx46 in nonosteoblastic cells.

In contrast with osteoblasts, Cx46 was present at the cell surface of HeLa/Cx46 cells, as well as in intracellular compartments (Fig. 4 *c*). While these cells were not extensively coupled, Cx46 expressed by HeLa/Cx46 cells formed functional gap junction channels, as determined by intercellular transfer of microinjected Lucifer yellow (Fig. 5). Texas red ovalbumin did not transfer between HeLa/Cx46 cells. This indicates that retention of Cx46 in an intracellular compartment depends upon the cell type examined. Furthermore, since Cx46 was readily detected at the surface of HeLa/Cx46 cells, it is likely that accumulation of appreciable amounts of Cx46 on the osteoblast cell surface would be visible by immunofluorescence microscopy. However, this does not rule out the possibility that Cx46 is transported to the cell surface and rapidly cleared by reinternalization.

The expression of Cx46 by transfected HeLa cells was also examined by immunoblotting (Fig. 4 *a*). HeLa/Cx46 cells showed both the 68- and 53-kD forms of Cx46 that are found associated with lens. This contrasts with results obtained with osteoblastic cells, where only the lower molecular mass form was present (Fig. 3). Thus, the ability to produce the 68-kD form of Cx46 correlated with the ability to form gap junctions containing Cx46. Whether one process is a prerequisite for the other is not known at present.

### Cx46 Is Retained in the TGN

The identity of the intracellular compartment containing Cx46 was determined with a series of fluorescence colocalization experiments in ROS cells. To label endocytic compartments, cells were incubated at 37°C for 1 h with medium containing the fluorescent fluid phase marker, Lucifer yellow. ROS cells labeled in this manner were fixed and immunostained for Cx46, and then examined by fluorescence microscopy. In these double-labeled cells, fluorescently labeled endocytic compartments and intracellular vesicles containing Cx46 showed distinct intracellular distributions (Fig. 6, *a* and *b*).

ER in fixed and permeabilized cells was preferentially labeled using a fluorescent lectin, fluorescein-conjugated concanavalin A (FITC-ConA), which recognizes the high mannose core oligosaccharide component of glycoproteins. Areas of the ER that are prominently labeled with FITC-ConA, such as the nuclear envelope and lattices in the periphery of the cell, showed little labeling for Cx46 (Fig. 6, *c* and *d*).

The Cx46-containing compartment in ROS cells colocalized with the Golgi apparatus by double-labeling immunofluorescence using a marker for the medial-Golgi stack (anti-GCI) (9). As shown in Fig. 7, *a* and *b*, both the anti-GCI and Cx46 showed prominent perinuclear localization.

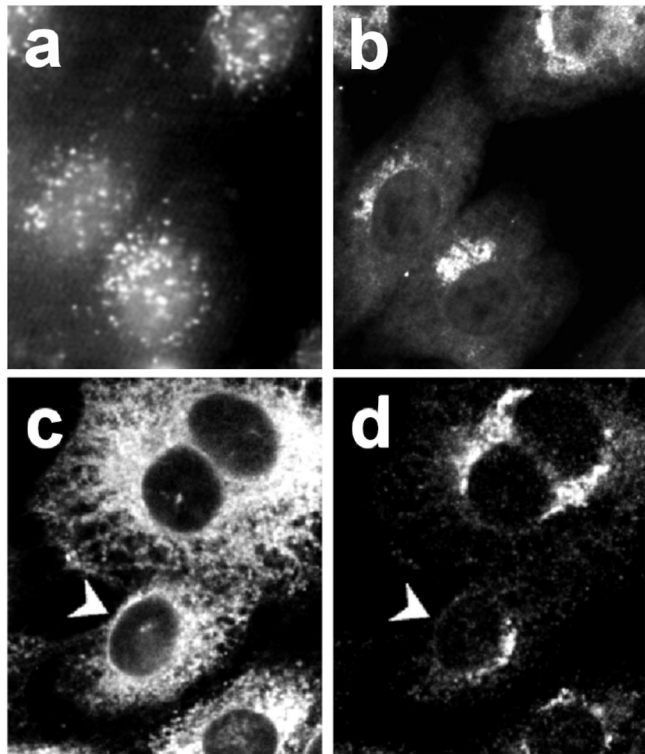


**Figure 6.** Cx46 is not localized to either endocytic or ER compartments. (*a* and *b*) ROS cells on glass coverslips were incubated for 1 h at 37°C in medium containing 10 mg/ml Lucifer yellow to label endocytic compartments (*a*). The cells were then fixed with paraformaldehyde, permeabilized using 0.2% Triton X-100, immunostained for Cx46 (*b*), and visualized by epifluorescence microscopy. The intracellular distribution of Lucifer yellow was distinct from the pattern observed for Cx46. (*c* and *d*) ROS cells on glass coverslips were fixed and permeabilized using methanol/acetone (50/50) and labeled with FITC-ConA (*c*). The cells were then immunostained using anti-Cx46 antiserum and rhodamine-conjugated goat anti-rabbit IgG (*d*). *c* and *d* were obtained by confocal microscopy. Colocalization between Cx46 and FITC-ConA, which preferentially labeled elements of the ER, was limited. In particular, note that low levels of Cx46 labeling were present in the nuclear envelope (*arrowhead*).

However, these two proteins were in distinct compartments. This was revealed by treatment of the cells with brefeldin A (BFA), which preferentially disassembles *cis* and medial aspects of the Golgi apparatus (54). When ROS cells were preincubated for 5 min with BFA and then fixed and examined by immunofluorescence, the GCI marker redistributed to the periphery of the cell, while the Cx46 staining pattern was relatively intact (Fig. 7, *c* and *d*). This suggests that Cx46 was located in a secretory compartment beyond the medial Golgi, either the *trans*-Golgi cistern or the TGN.

To further examine this possibility, we performed colocalization experiments using a monoclonal anti-rat TGN38 antibody (24). As shown in Fig. 7, *e* and *f*, both Cx46 and TGN38 colocalize to the perinuclear region of the cell. The distribution of these two proteins was not affected by short-term treatment with BFA (not shown). However, in cells incubated for 30 min in the presence of BFA, both Cx46 and TGN38 condensed into the same concentrated spot in

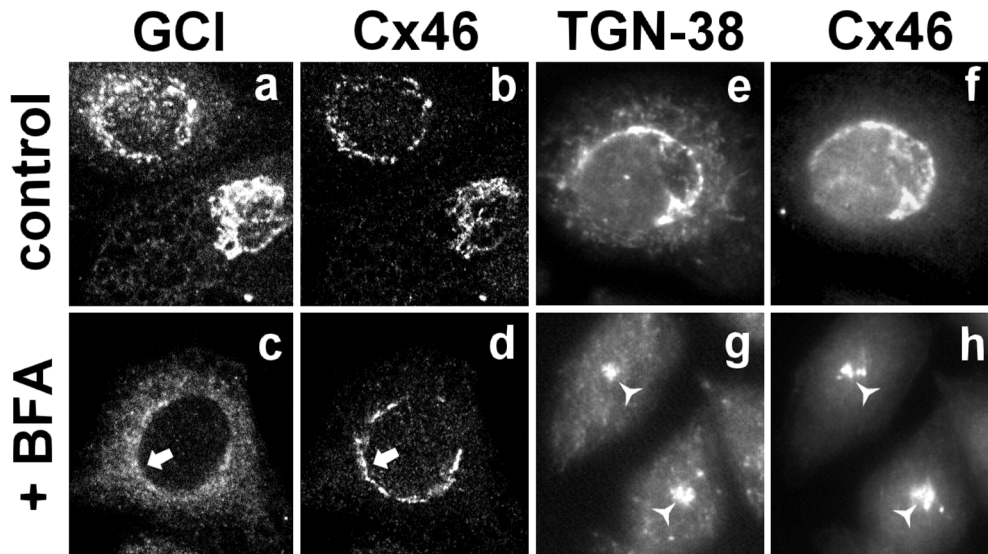


**Figure 7.** Cx46 is in a *trans*-Golgi compartment. (a and b) ROS cells on glass coverslips were fixed, permeabilized, and immunolabeled with mAbs that recognize a medial-Golgi protein (*GCI*). The cells were also immunostained for Cx46 using polyclonal antiserum, and then labeled with rhodamine-conjugated goat anti-mouse IgG (a) and FITC-conjugated goat anti-rabbit IgG (b). (c and d) ROS cells on glass coverslips were preincubated in MEM containing 10  $\mu$ g/ml brefeldin A (*BFA*) for 5 min at 37°C. The cells were then fixed, permeabilized, and immunolabeled for *GCI* (c) and Cx46 (d). a–d were obtained

by confocal microscopy. While *BFA* disrupts the medial Golgi, Cx46 remains in the perinuclear region (arrow). (e and f) ROS cells on glass coverslips were fixed, permeabilized, and immunolabeled with mAbs that recognize TGN38 (e) and Cx46 using polyclonal antiserum (f). (g and h) ROS cells on glass coverslips were preincubated in MEM containing 10  $\mu$ g/ml *BFA* for 30 min at 37°C. The cells were then fixed, permeabilized, and immunolabeled for TGN38 (g) and Cx46 (h). e–h were obtained by epifluorescence microscopy. Under these conditions, both proteins condense into a dot in the center of the cell (arrowheads).

the nuclear region (Fig. 7, g and h). This is similar to the pattern of TGN38 labeling in normal rat kidney (NRK) cells treated for 30–60 min with *BFA* (34, 48). Taken together, these observations suggest that the intracellular pool of Cx46 likely corresponds to an aspect of the TGN.

We attempted to stimulate the transport of Cx46 to the plasma membrane by plating osteoblastic cells under a variety of culture conditions. Under the conditions examined, little, if any, Cx46 was found to be localized to the cell surface. We also incubated ROS cells for short periods (2–12 h) before immunofluorescence labeling with a number of agents known to affect bone cell metabolism (47), such as  $\beta$ -glycerophosphate (2.3–5.8 mM) + ascorbate (0.1–0.25 mg/ml), dexamethasone (10–250  $\mu$ M), PMA (0.1  $\mu$ M)  $\pm$  bromo-A23187 (0.1  $\mu$ g/ml), parathyroid hormone (0.125–1.0  $\mu$ M),  $\beta$ -estradiol (0.5–50  $\mu$ g/ml), 1,25-dihydroxy-vitamin D<sub>3</sub> (5–25 ng/ml), and dibutyryl-cAMP (0.1 mM), as well as a variety of plating densities and mechanical stress. None of these treatments altered the intracellular distribution of Cx46 in ROS cells.

#### Osteoblasts Retain Cx46 as a Monomer

To examine the assembly of Cx43 and Cx46, we used techniques previously described by Musil and Goodenough (40) using 1% Triton X-100 at 4°C, conditions that enable the solubilization of intact Cx43 hexamers in other cell types. Cx43 and Cx46 were solubilized to different extents (Fig. 8). Note that Cx43 already assembled into gap junctional plaques is resistant to solubilization under these conditions (39). As determined by immunoprecipitation analysis, ~50% of the Cx43 in ROS cells was soluble in 1% Triton X-100 at 4°C, while virtually all of the Cx46 was solubilized under the same conditions.

Detergent-extracted connexin preparations were resolved into monomers and multimers by sucrose gradient

velocity sedimentation (Fig. 9). Cx43 from ROS cells resolved into two fractions. The major fraction centered at 8% sucrose corresponds to Cx43 monomers, while the peak at 15% sucrose corresponds to multimers. Multimeric

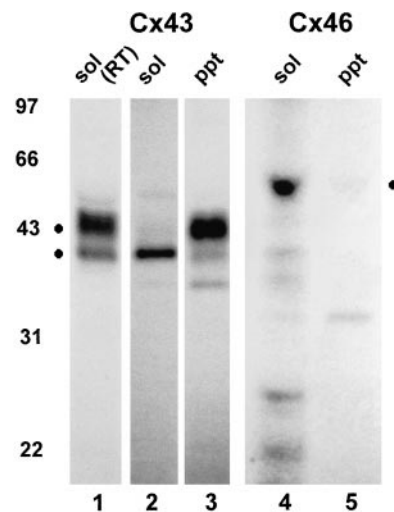


**Figure 8.** Triton solubility of Cx43 and Cx46 in ROS cells. ROS cells were metabolically radiolabeled with <sup>35</sup>S-Trans label, harvested, homogenized, and solubilized in 1% Triton X-100 at either room temperature (lane 1) or 4°C (lanes 2–5) for 30 min. Triton-soluble (lanes 1, 2, and 4) and -insoluble (lanes 3 and 5) fractions were analyzed by immunoprecipitation using antisera that recognizes either Cx43 (lanes 1–3) or Cx46 (lanes 4 and 5). Note that the Cx46 band (lane 4) was somewhat distorted due to the presence of high levels of IgG heavy chain required for immunoprecipitation. At 4°C, Cx46 showed complete Triton X-100 solubility, while Cx43 was only partially soluble (lane 2). Migration of molecular weight standards is indicated in the figure, and dots correspond to specific protein bands.

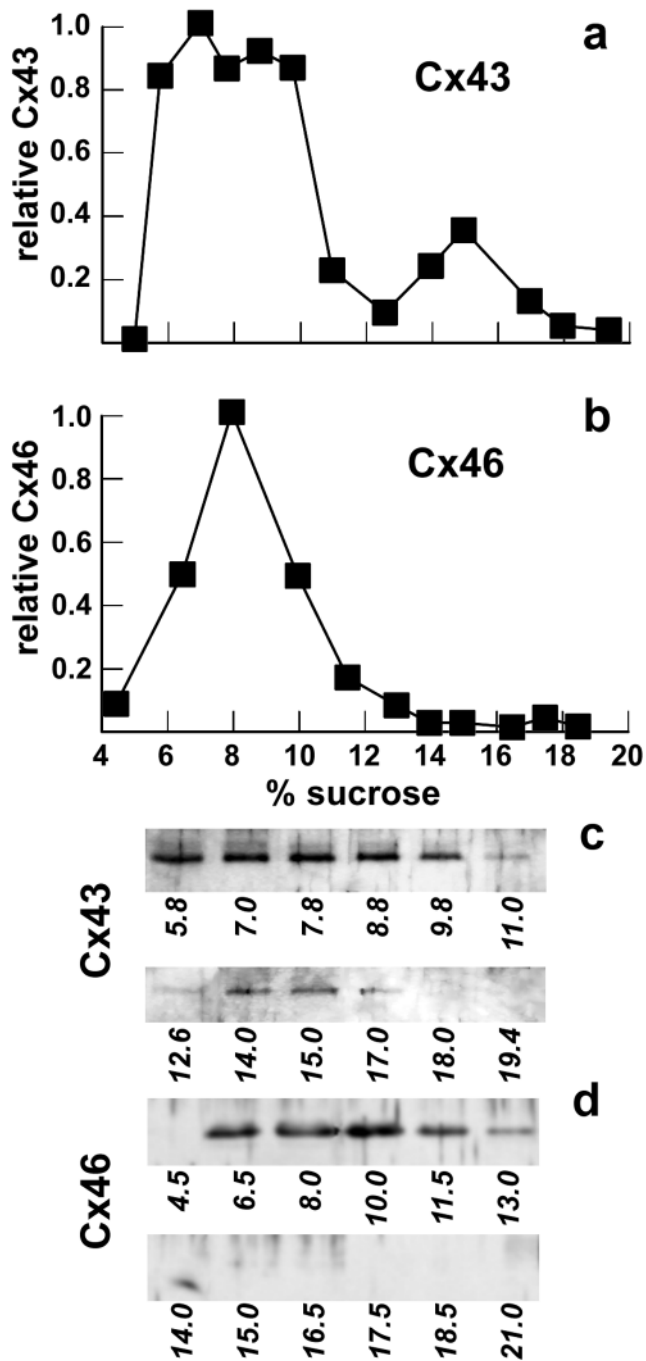


**Figure 9.** Sucrose gradient analysis of Cx43 and Cx46 oligomerization. ROS cells were harvested and homogenized, and Triton X-100 was added to a final concentration of 1%. After an incubation for 30 min at 4°C, the preparation was centrifuged at 50,000 *g* for 30 min, and the resulting Triton-soluble fraction was layered onto a 5–20% sucrose gradient containing 0.1% Triton X-100 (with a 25% sucrose cushion). The gradient was centrifuged for 16 h at 148,000 *g*. Fractions were collected from the bottom of the tube, diluted 1:1 with sample buffer, resolved by SDS-PAGE, and electrophoretically transferred to PVDF membranes. Cx43 (a and c) and Cx46 (b and d) were detected by immunoblotting (c and d) and quantified by densitometry (a and b). Lanes in c and d are labeled with the corresponding sample sucrose concentration, which was determined by refractometry.

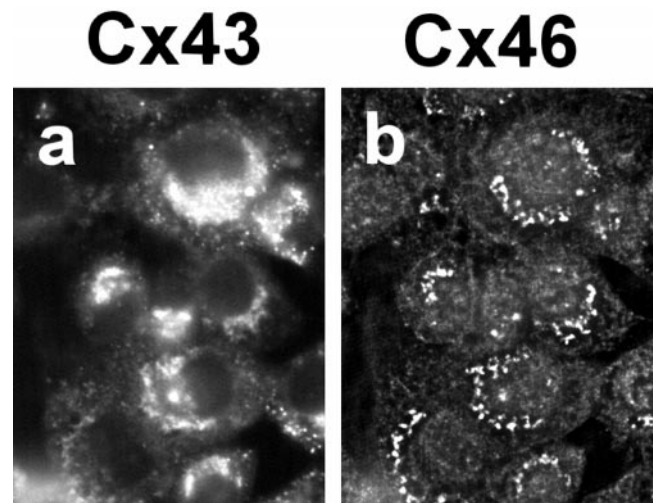


**Figure 10.** Cx43 and Cx46 are retained in the same compartment in the presence of monensin. ROS cells on glass coverslips were preincubated in MEM containing 10  $\mu$ M monensin for 4 h at 37°C. The cells were then fixed, permeabilized, and immunolabeled for Cx43 (a) and Cx46 (b) as described in Fig. 1.

Cx43 consisted of  $21.4 \pm 2.8\%$  ( $n = 3$ ) of the total Triton X-100-soluble Cx43. The preponderance of Cx43 monomers over hexamers was expected, since the Triton-soluble fraction of Cx43 is likely to contain mostly newly synthesized Cx43 (39, 40). However, some monomeric Cx43 may be due to spontaneous disassembly of hexameric Cx43 during the course of the experiment.

Treatment of NRK cells with BFA inhibits the oligomerization of Cx43, suggesting that Cx43 is assembled into oligomers in a late Golgi apparatus compartment (40). If this is the case, then treatment of ROS cells with monensin, which inhibits *cis* to medial transport through the Golgi apparatus, should also inhibit Cx43 oligomerization. As shown by immunofluorescence microscopy in Fig. 10, monensin-treated ROS cells showed Cx43 and Cx46 retained in a similar perinuclear region of the cell. This is consistent with results obtained with monensin-treated cardiac myocytes (45). When oligomerization of Cx43 was examined in monensin-treated cells, only 8% ( $n = 2$ ) of the Triton-soluble Cx43 isolated from monensin-treated cells was assembled into multimers, as compared with control cells that had two- to threefold more Cx43 in the hemichannel form (Fig. 11). Also, since we could detect this difference in the amount of Cx43 assembled into hemichannels, it is likely that nonspecific aggregation of Cx43 did not occur during the solubilization and sucrose gradient fractionation procedure.

In contrast with Cx43, Cx46 solubilized from ROS cells migrated as a single peak centered at 8% sucrose (Fig. 9 b). Since nearly all of the Cx46 was soluble in 1% Triton X-100, this suggests that all of the Cx46 was being retained by ROS cells in a monomeric form.

One possible concern in using Triton X-100-solubilized preparations is that Cx46-containing oligomers may not be stable under these conditions. To examine this possibility, we prepared Triton X-100-soluble extracts from both HeLa/Cx46 cells and whole rat lens. While HeLa/Cx46 cells were solubilized using the same conditions used for ROS

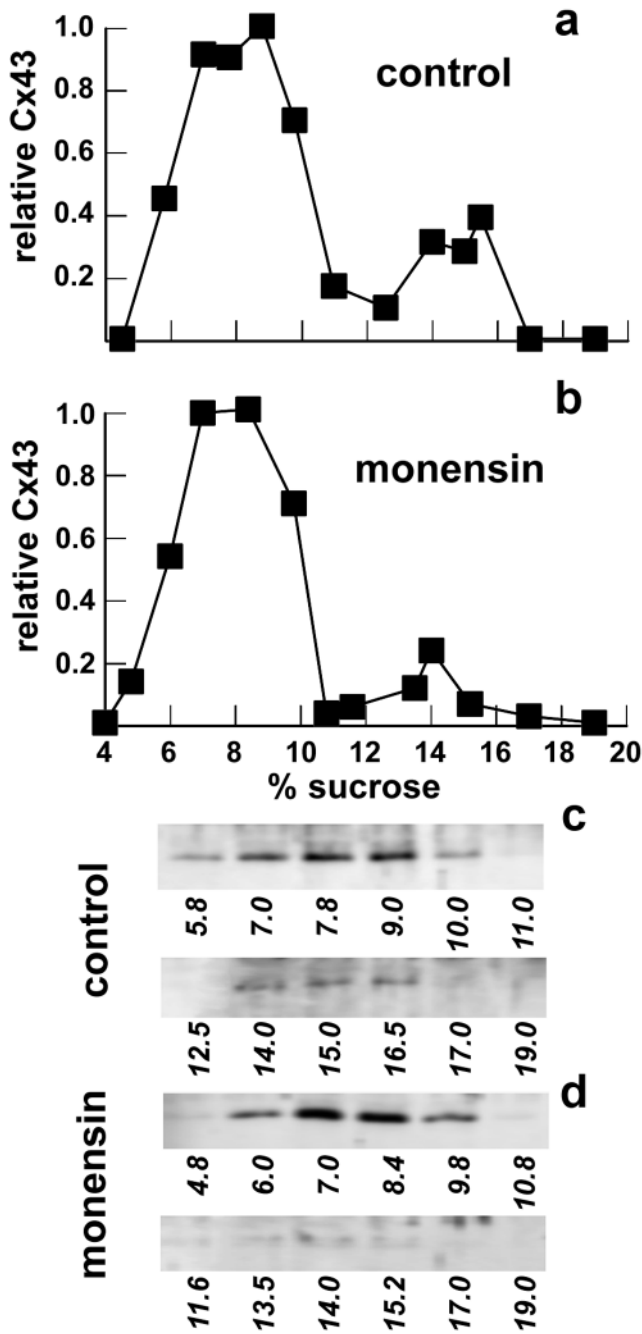


**Figure 11.** Monensin inhibits Cx43 oligomerization in ROS cells. Cells were incubated in either the absence (a) or presence (b) of 10  $\mu$ M monensin for 4 h at 37°C. The cells were then harvested and homogenized, and Triton X-100 was added to a final concentration of 1%. After an incubation for 30 min at 4°C, the preparation was centrifuged at 50,000 g for 30 min, and the resulting supernatant was analyzed by sucrose gradient fractionation as described above. Cx43 in control (a and c) and monensin-treated (b and d) cells were detected by immunoblotting (c and d) and quantified by densitometry (a and b). Monensin treatment, which inhibits transport from the *cis*- to medial-Golgi compartments, also inhibited Cx43 oligomerization.

cells, extensive incubation with 1% Triton X-100 at 4°C was required to solubilize detectable amounts of material from rat lens. Both the 53- and 68-kD forms of Cx46 were solubilized under these conditions (Figs. 12 and 13).

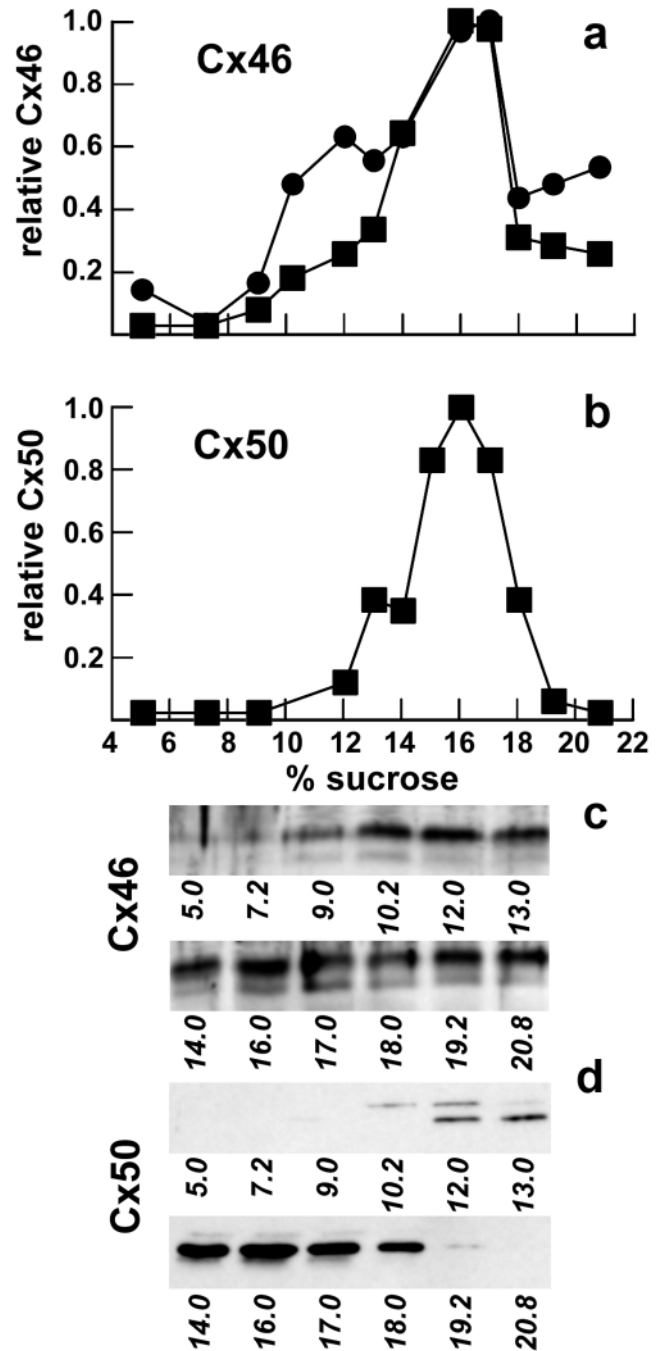


**Figure 12.** Connexin hemichannels from rat lens are stable in Triton X-100. Connexins solubilized from rat lenses were analyzed by sucrose gradient fractionation as described above. Cx46 (a and c) and Cx50 (b and d) were detected by immunoblotting and quantified by densitometry (a and b). Symbols in a correspond to measurements of total Cx46 (●) and the 53-kD form of Cx46 (■).

When Triton X-100-soluble extracts from lens were examined by sucrose gradient fractionation, the majority of the Cx46 was found to be in oligomeric forms (Fig. 12 a). We also examined this gradient for Cx50, another abundant lens connexin (14, 15). The profile for Cx50 was very comparable to that observed for Cx46 in lens (Fig. 12 b). Similar results were obtained by sucrose gradient analysis of Cx46 solubilized from HeLa/Cx46 cells, although the

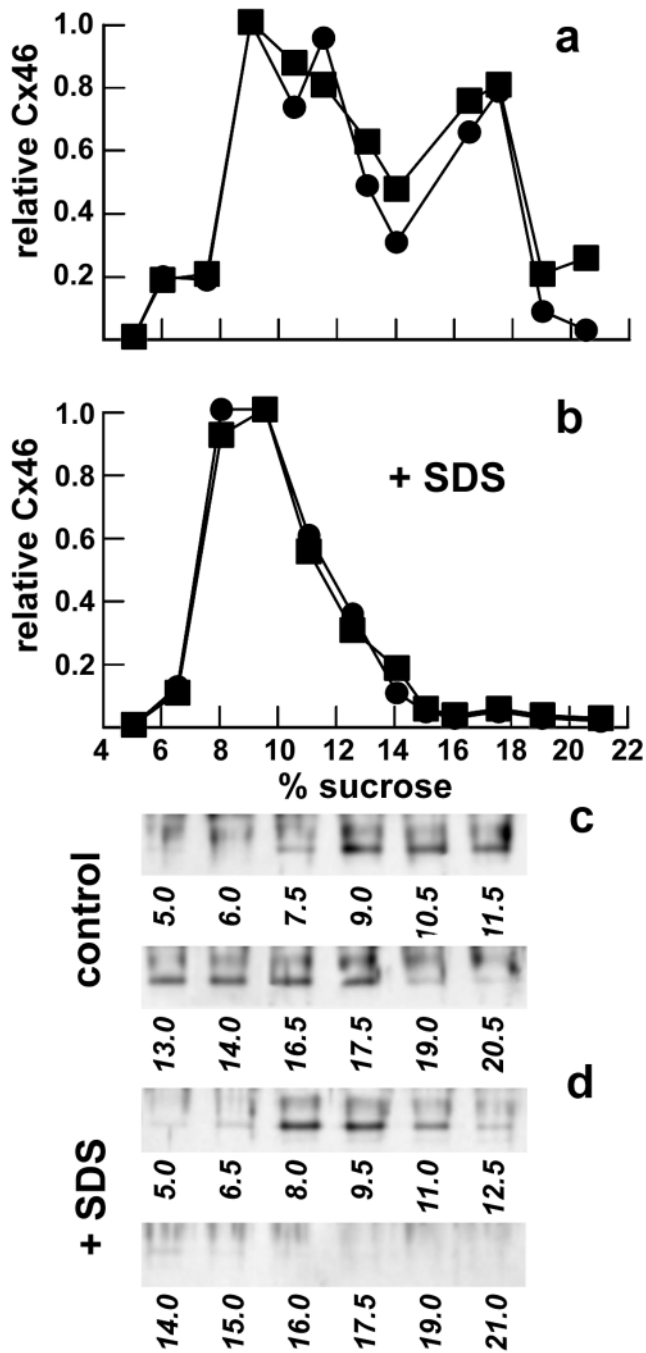


**Figure 13.** Connexin hemichannels from HeLa/Cx46 cells are stable in Triton X-100. Connexins solubilized from HeLa/Cx46 cells were further incubated at 4°C for 1 h in either the absence (*a* and *c*) or presence (*b* and *d*) of 0.2% SDS, and then analyzed by sucrose gradient fractionation as described above. Symbols correspond to measurements of total Cx46 (●) and the 53-kD form of Cx46 (■). In the presence of SDS, Cx46 oligomers dissociated into monomers that migrated on the sucrose gradient as a single peak centered at 8–9% sucrose.

peak at 14–18% was significantly reduced (Fig. 13 *a*). The sucrose gradient profiles of Cx46 isolated from lens and HeLa/Cx46 cells are consistent with the notion that multimers containing Cx46 were largely stable in the presence of Triton X-100. This is further supported by Fig. 13 *b*,

where Cx46 extracted from HeLa/Cx46 cells and then dissociated by treatment with 0.2% SDS migrated on the gradient as a single peak at 8–9% sucrose.

### Discussion

In this paper we have examined the expression of Cx46 by osteoblastic, lens, and transfected HeLa cells. Osteoblastic cells retained Cx46 as a monomer in an intracellular compartment that is likely to be an aspect of the TGN. In contrast, Cx46 was assembled into oligomers by lens and HeLa/Cx46 cells and transported to the cell surface. This raises the possibility that connexin assembly and transport are interlinked and regulated processes.

Connexins are assembled into a hemichannel in an intracellular compartment before transport to the plasma membrane (33, 40). This hemichannel then pairs with another hemichannel on a neighboring cell to form a complete gap junction channel. There is evidence supporting both ER and Golgi apparatus as sites for connexin oligomerization. Kumar et al. (33) have found by EM that BHK cells transfected with Cx32 ( $\beta_1$ ) form intracellular gap junctional structures in the ER as well as the plasma membrane. This indicates that Cx32 assembly into hemichannels also occurred at the ER and is consistent with “classical” models for transmembrane protein assembly (3, 13, 28). An alternative model has been proposed by Musil and Goodenough (40). Using sucrose gradient fractionation to analyze connexin assembly, they found that Cx43 is assembled in a late Golgi compartment of NRK and CHO cells, most likely the TGN. When cells were treated with BFA, oligomerization was inhibited. Similar results were obtained using temperature-sensitive mutant cell lines deficient in ER to Golgi transport.

We used sucrose gradient fractionation to examine the oligomerization state of Cx43 and Cx46 present in Triton X-100 extracts. Treatment of ROS cells with monensin, which inhibited *cis*- to medial-Golgi transport, also reduced Cx43 hemichannel formation by >62% (Fig. 10). While this evidence is not conclusive, it is consistent with a *trans*-Golgi compartment as the site of Cx43 oligomerization in this system. Since Cx43 assembly was not completely inhibited, it is possible that Cx43 hemichannels may also be assembled in the ER. Alternatively, some of the hemichannels that we detected in the presence of monensin may be due to Cx43 disassembled from gap junctions that is en route to degradation.

We found that Cx46 oligomers were stable in Triton X-100 (Figs. 12 and 13). Sucrose gradients have also been used to analyze connexin channels isolated from ovine lens (25). Analogous to chick, ovine, and bovine lens (25, 29), it is likely that most hemichannels isolated from rat lens contained Cx50 in addition to Cx46. Preliminary analysis of ROS and UMR cells indicates that these cells do not express Cx50 (not shown). An absolute requirement for Cx50 is not likely for Cx46 incorporation into gap junction channels, since we found that HeLa/Cx46 cells were able to form functional gap junctions in the absence of Cx50, albeit at relatively low levels. Formation of gap junctions purely from Cx46 has also been described in other systems (59, 60).

Cx46 was retained in a monomer, rather than a hemichannel form, by ROS cells. Based on colocalization experiments shown above, it seems likely that osteoblasts transported Cx46 to compartments where connexin oligomerization occurs. This is consistent with a requirement for connexin oligomerization as a prerequisite for transport from the TGN and/or retention at the cell surface. The notion of quality control at the level of the Golgi apparatus is supported by the observation that some mutant viral glycoproteins exit the ER without being properly assembled, but are retained in the Golgi apparatus (20, 42).

Immunofluorescence was used to determine whether Cx46 was present at the plasma membrane of osteoblastic cells. This technique does not completely rule out the possibility that Cx46 transport to the cell surface occurs, but suggests that it is rapidly reinternalized after delivery to the plasma membrane. TGN38 (48) and furin (37, 56) are examples of proteins that continuously recycle at low levels between the TGN and plasma membrane, yet are not readily detectable at the cell surface by conventional indirect immunofluorescence. Furthermore, the communication-deficient cell lines L929 and S180, which do not show accumulation of Cx43 at the plasma membrane by immunofluorescence (41), contain a pool of Cx43 that is accessible by surface biotinylation (39). Interestingly, S180 and L929 cells show low levels of Cx43 phosphorylation (41), analogous to our observations with Cx46 in osteoblasts. However, these situations are not completely comparable, since both S180 and L929 cells assemble Cx43 into hemichannels (40). Cx43 hemichannels at the cell surface have also been observed in other systems (35).

It is also possible that Cx46 is transported by osteoblasts along a regulated secretory pathway that is distinct from the transport pathway for Cx43. Rat uterine myometrial cells provide a precedent for the stimulated transport of connexins to form gap junctions (2, 10, 19, 23, 44). Whether the intracellular compartment containing Cx46 is a regulated secretory compartment is not known at present. However, storage vesicles that accumulate other transmembrane proteins subject to stimulated transport to the plasma membrane, such as GLUT4, accumulate in the perinuclear region in other cell types (27, 36).

Since Cx43 and Cx46 had distinct intracellular distributions in osteoblastic cells, this indicates that these two connexins were not randomly intermixing in these cells. It is not known whether Cx43 and Cx46 can form heteromeric channels in other systems, and there is no a priori reason that these two  $\alpha$ -connexins cannot intermix. In fact, Cx43 has been observed to colocalize near lens gap junctional plaques that also contain Cx46 (14). Also, Cx43 and Cx46 expressed by *Xenopus* oocytes can form functional heterotypic channels (55, 59).

Since Cx43 and Cx46 have different fates in osteoblastic cells, our data support the notion that connexin transport is a specific process and not due to the bulk flow of connexins along a "default" secretory pathway. Also, oligomerization seems to be interconnected with connexin targeting and transport to the cell surface. Further work will be required to find structural determinants that either target connexins to specific intracellular locations or control connexin transport at the level of gap junction channel assembly.

We are grateful to Dr. S. Kornfeld and the anonymous reviewers for their very helpful comments. We also thank A. Robertson for technical assistance with the RNA blot and Dr. R. Civitelli for providing calvarial cells.

This research was supported in part by National Institutes of Health grants GM45815 and DK46686.

Received for publication 27 June 1996 and in revised form 2 April 1997.

## References

- Balch, W.E., and J.E. Rothman. 1985. Characterization of protein transport between successive compartments of the Golgi apparatus: asymmetric properties of donor and acceptor activities in a cell-free system. *Arch. Biochem. Biophys.* 240:413-425.
- Balducci, J., B. Risek, N.B. Gilula, A. Hand, J.F. Egan, and A.M. Vintzileos. 1993. Gap junction formation in human myometrium: a key to preterm labor? *Am. J. Obstet. Gynecol.* 168:1609-1615.
- Bergeron, J.J.M., M.B. Brenner, D.Y. Thomas, and D.B. Williams. 1994. Calnexin: a membrane-bound chaperone of the endoplasmic reticulum. *Trends Biochem. Sci.* 19:124-128.
- Beyer, E.C., and T.H. Steinberg. 1991. Evidence that the gap junction protein connexin-43 is the ATP-induced pore of mouse macrophages. *J. Biol. Chem.* 266:7971-7974.
- Brissette, J.L., N.M. Kumar, N.B. Gilula, J.E. Hall, and G.P. Dotto. 1994. Switch in gap junction protein expression is associated with selective changes in junctional permeability during keratinocyte differentiation. *Proc. Natl. Acad. Sci. USA.* 91:6453-6457.
- Bruzzone, R., T.W. White, and D.A. Goodenough. 1996. The cellular internet: on-line with connexins. *Bioessays.* 18:709-718.
- Bruzzone, R., T.W. White, and D.L. Paul. 1996. Connections with connexins: the molecular basis of direct intercellular signalling. *Eur. J. Biochem.* 238:1-27.
- Carel, J.C., B. Frazier, T.J. Ley, and V.M. Holers. 1989. Analysis of epitope expression and the functional repertoire of recombinant complement receptor 2 (CR2/CD21) in mouse and human cells. *J. Immunol.* 143:923-930.
- Chicheportiche, Y., and A.M. Tartakoff. 1987. Monoclonal antibodies as markers of the endocytic and secretory pathways. *Eur. J. Cell Biol.* 44:135-143.
- Chow, L., and S.J. Lye. 1994. Expression of the gap junction protein connexin-43 is increased in the human myometrium toward term and with the onset of labor. *Am. J. Obstet. Gynecol.* 170:788-795.
- Civitelli, R., E.C. Beyer, P.M. Warlow, A.J. Robertson, S.T. Geist, and T.H. Steinberg. 1993. Connexin43 mediates direct intercellular communication in human osteoblastic cell networks. *J. Clin. Invest.* 91:1888-1896.
- Darrow, B.J., J.G. Laing, P.D. Lampe, J.E. Saffitz, and E.C. Beyer. 1995. Expression of multiple connexins in cultured neonatal rat ventricular myocytes. *Circ. Res.* 76:381-387.
- Doms, R.W., R.A. Lamb, J.K. Rose, and A. Helenius. 1993. Folding and assembly of viral membrane glycoproteins. *Virology.* 193:545-562.
- Donaldson, P.J., Y. Dong, M. Roos, C. Green, D.A. Goodenough, and J. Kistler. 1995. Changes in lens connexin expression lead to increased gap junctional voltage dependence and conductance. *Am. J. Physiol.* 269:590-600.
- Dong, Y., M. Roos, T. Gruijters, P. Donaldson, S. Bullivant, E. Beyer, and J. Kistler. 1994. Differential expression of two gap junction proteins in corneal epithelium. *Eur. J. Cell Biol.* 64:95-100.
- Elfgang, C., R. Eckert, H. Lichtenberg-Frate, A. Butterweck, O. Traub, R.A. Klein, D.F. Hulser, and K. Willecke. 1995. Specific permeability and selective formation of gap junction channels in connexin-transfected HeLa cells. *J. Cell Biol.* 129:805-817.
- Evans, W.H. 1994. Assembly of gap junction intercellular communication channels. *Biochem. Soc. Trans.* 22:788-792.
- Falk, M.M., N.M. Kumar, and N.B. Gilula. 1994. Membrane insertion of gap junction connexins: polytopic channel forming membrane proteins. *J. Cell Biol.* 127:343-355.
- Garfield, R.E., and E.L. Hertzberg. 1990. Cell-to-cell coupling in the myometrium: Emil Bozler's prediction. *Prog. Clin. Biol. Res.* 327:673-681.
- Garten, W., C. Will, K. Buckard, K. Kuroda, D. Ortman, K. Munk, C. Scholtissek, H. Schnittler, D. Drenkhahn, and H.D. Klenk. 1992. Structure and assembly of hemagglutinin mutants of fowl plague virus with impaired surface transport. *J. Virol.* 66:1495-1505.
- Goodenough, D.A., J.A. Goliger, and D.L. Paul. 1996. Connexins, connexons and intercellular communication. *Annu. Rev. Biochem.* 65:475-502.
- Gupta, V.K., V.M. Berthoud, N. Atal, J.A. Jarillo, L.C. Barrio, and E.C. Beyer. 1994. Bovine connexin44, a lens gap junction protein: molecular cloning, immunologic characterization, and functional expression. *Invest. Ophthalmol. Vis. Sci.* 35:3747-3758.
- Hendrix, E.M., S.J. Mao, W. Everson, and W.J. Larsen. 1992. Myometrial connexin 43 trafficking and gap junction assembly at term and in preterm labor. *Mol. Reprod. Dev.* 33:27-38.
- Horn, M., and G. Banting. 1994. Okadaic acid treatment leads to a fragmentation of the trans-Golgi network and an increase in expression of TGN38 at the cell surface. *Biochem. J.* 301:69-73.

25. Jiang, J.X., and D.A. Goodenough. 1996. Heteromeric connexons in lens gap junction channels. *Proc. Natl. Acad. Sci. USA* 93:1287–1291.
26. Jiang, J.X., D.L. Paul, and D.A. Goodenough. 1993. Posttranslational phosphorylation of lens fiber connexin46: a slow occurrence. *Invest. Ophthalmol. Vis. Sci.* 34:3558–3565.
27. Kanai, F., Y. Nishioka, H. Hayashi, S. Kamohara, M. Todaka, and Y. Ebina. 1993. Direct demonstration of insulin-induced GLUT4 translocation to the surface of intact cells by insertion of a c-myc epitope into an exofacial GLUT4 domain. *J. Biol. Chem.* 268:14523–14526.
28. Klausner, R.D. 1989. Architectural editing: determining the fate of newly synthesized membrane proteins. *New Biol.* 1:3–8.
29. König, N., and G.A. Zampighi. 1995. Purification of bovine lens cell-to-cell channels composed of Connexin44 and Connexin50. *J. Cell Sci.* 108:3091–3098.
30. Koval, M., S.T. Geist, E.M. Westphale, A.E. Kemendy, R. Civitelli, E.C. Beyer, and T.H. Steinberg. 1995. Transfected connexin45 alters gap junction permeability in cells expressing endogenous connexin43. *J. Cell Biol.* 130:987–995.
31. Kren, B.T., N.M. Kumar, S.Q. Wang, N.B. Gilula, and C.J. Steer. 1993. Differential regulation of multiple gap junction transcripts and proteins during rat liver regeneration. *J. Cell Biol.* 123:707–718.
32. Kumar, N.M., and N.B. Gilula. 1996. The gap junction communication channel. *Cell.* 84:381–388.
33. Kumar, N.M., D.S. Friend, and N.B. Gilula. 1995. Synthesis and assembly of human  $\beta 1$  gap junctions in BHK cells by DNA transfection with the human  $\beta 1$  cDNA. *J. Cell Sci.* 108:3725–3734.
34. Ladinsky, M.S., and K.E. Howell. 1992. The trans-Golgi network can be dissected structurally and functionally from the cisternae of the Golgi complex by brefeldin. *Eur. J. Cell Biol.* 59:92–105.
35. Li, H.Y., T.F. Liu, A. Lazrak, C. Peracchia, G.S. Goldberg, P.D. Lampe, and R.G. Johnson. 1996. Properties and regulation of gap junctional hemichannels in the plasma membranes of cultured cells. *J. Cell Biol.* 134:1019–1030.
36. Marsh, B.J., R.A. Alm, S.R. McIntosh, and D.E. James. 1995. Molecular regulation of GLUT-4 targeting in 3T3-L1 adipocytes. *J. Cell Biol.* 130:1081–1091.
37. Molloy, S.S., L. Thomas, J.K. VanSlyke, P.E. Stenberg, and G. Thomas. 1994. Intracellular trafficking and activation of the furin proprotein convertase: localization to the TGN and recycling from the cell surface. *EMBO (Eur. Mol. Biol. Organ.) J.* 13:18–33.
38. Musil, L.S., and D.A. Goodenough. 1990. Gap junctional intercellular communication and the regulation of connexin expression and function. *Curr. Opin. Cell Biol.* 2:875–880.
39. Musil, L.S., and D.A. Goodenough. 1991. Biochemical analysis of connexin43 intracellular transport, phosphorylation, and assembly into gap junctional plaques. *J. Cell Biol.* 115:1357–1374.
40. Musil, L.S., and D.A. Goodenough. 1993. Multisubunit assembly of an integral plasma membrane channel protein, gap junction connexin43, occurs after exit from the ER. *Cell.* 74:1065–1077.
41. Musil, L.S., B.A. Cunningham, G.M. Edelman, and D.A. Goodenough. 1990. Differential phosphorylation of the gap junction protein connexin43 in junctional communication-competent and -deficient cell lines. *J. Cell Biol.* 111:2077–2088.
42. Naruse, H., C. Scholtissek, and H.D. Klenk. 1986. Temperature-sensitive mutants of fowl plague virus defective in the intracellular transport of the hemagglutinin. *Virus Res.* 5:293–305.
43. Paul, D.L., L. Ebihara, L.J. Takemoto, K.I. Swenson, and D.A. Goodenough. 1991. Connexin46, a novel lens gap junction protein, induces voltage-gated currents in nonjunctional plasma membrane of *Xenopus* oocytes. *J. Cell Biol.* 115:1077–1089.
44. Petrocelli, T., and S.J. Lye. 1993. Regulation of transcripts encoding the myometrial gap junction protein, connexin-43, by estrogen and progesterone. *Endocrinology.* 133:284–290.
45. Puranam, K.L., D.W. Laird, and J.P. Revel. 1993. Trapping an intermediate form of connexin43 in the Golgi. *Exp. Cell Res.* 206:85–92.
46. Rahman, S., G. Carlile, and W.H. Evans. 1993. Assembly of hepatic gap junctions. Topography and distribution of connexin 32 in intracellular and plasma membranes determined using sequence-specific antibodies. *J. Biol. Chem.* 268:1260–1265.
47. Raisz, L.G., and G.A. Rodan. 1990. Cellular basis for bone turnover. In *Metabolic Bone Disease and Clinically Related Disorders*. L.V. Avioli and S.M. Krane, editors. W.B. Saunders, Co., Philadelphia, PA. 1–41.
48. Reaves, B., M. Horn, and G. Banting. 1993. TGN38/41 recycles between the cell surface and the TGN: brefeldin A affects its rate of return to the TGN. *Mol. Biol. Cell.* 4:93–105.
49. Reynhout, J.K., P.D. Lampe, and R.G. Johnson. 1992. An activator of protein kinase C inhibits gap junction communication between cultured bovine lens cells. *Exp. Cell Res.* 198:337–342.
50. Schiller, P.C., P.P. Mehta, B.A. Roos, and G.A. Howard. 1992. Hormonal regulation of intercellular communication: parathyroid hormone increases connexin 43 gene expression and gap-junctional communication in osteoblastic cells. *Mol. Endocrinol.* 6:1433–1440.
51. Schirrmacher, K., F. Brummer, R. Dusing, and D. Bingmann. 1993. Dye and electric coupling between osteoblast-like cells in culture. *Calcif. Tissue Int.* 53:53–60.
52. Stauffer, K.A. 1995. The gap junction proteins  $\beta 1$ -connexin (connexin32) and  $\beta 2$ -connexin (connexin26) can form heteromeric hemichannels. *J. Biol. Chem.* 270:6768–6772.
53. Steinberg, T.H., R. Civitelli, S.T. Geist, A.J. Robertson, E. Hick, R.D. Veenstra, H.Z. Wang, P.M. Warlow, E.M. Westphale, J.G. Laing et al. 1994. Connexin43 and connexin45 form gap junctions with different molecular permeabilities in osteoblastic cells. *EMBO (Eur. Mol. Biol. Organ.) J.* 13:744–750.
54. Strous, G.J., P. van Kerkhof, G. van Meer, S. Rijnboutt, and W. Stoorvogel. 1993. Differential effects of brefeldin A on transport of secretory and lysosomal proteins. *J. Biol. Chem.* 268:2341–2347.
55. Swenson, K.I., J.R. Jordan, E.C. Beyer, and D. L. Paul. 1989. Formation of gap junctions by expression of connexins in *Xenopus* oocyte pairs. *Cell.* 57:145–155.
56. Takahashi, S., T. Nakagawa, T. Banno, T. Watanabe, K. Murakami, and K. Nakayama. 1995. Localization of furin to the trans-Golgi network and recycling from the cell surface involves Ser and Tyr residues within the cytoplasmic domain. *J. Biol. Chem.* 270:28397–28401.
57. Tenbroek, E., M. Arneson, L. Jarvis, and C. Louis. 1992. The distribution of the fiber cell intrinsic membrane proteins MP20 and connexin46 in the bovine lens. *J. Cell Sci.* 103:245–257.
58. Veenstra, R.D., H.Z. Wang, E.M. Westphale, and E.C. Beyer. 1992. Multiple connexins confer distinct regulatory and conductance properties of gap junctions in developing heart. *Circ. Res.* 71:1277–1283.
59. White, T.W., R. Bruzzone, S. Wolfram, D.L. Paul, and D.A. Goodenough. 1994. Selective interactions among the multiple connexin proteins expressed in the vertebrate lens: the second extracellular domain is a determinant of compatibility between connexins. *J. Cell Biol.* 125:879–892.
60. White, T.W., D.L. Paul, D.A. Goodenough, and R. Bruzzone. 1995. Functional analysis of selective interactions among rodent connexins. *Mol. Biol. Cell.* 6:459–470.